


## Article

# Modification of Ti/Sb-SnO<sub>2</sub>/PbO<sub>2</sub> Electrode by Active Granules and Its Application in Wastewater Containing Copper Ions

Xuanqi Kang <sup>1,2,†</sup>, Jia Wu <sup>2,\*,†</sup>, Zhen Wei <sup>2</sup>, Bo Jia <sup>2</sup>, Qing Feng <sup>2</sup>, Shangyuan Xu <sup>2</sup> and Yunhai Wang <sup>1,\*</sup> 

<sup>1</sup> State Key Laboratory of Multiphase Flow in Power Engineering, Department of Environmental Science and Engineering, Xi'an Jiaotong University, Xi'an 710049, China

<sup>2</sup> Xi'an Taijin New Energy & Materials Sci-Tech Co., Ltd., Xi'an 710016, China

\* Correspondence: lhwu123456@126.com (J.W.); wang.yunhai@mail.xjtu.edu.cn (Y.W.);

Tel.: +86-15802900957 (J.W.); Fax: +86-29-86968411 (J.W.)

† These authors contributed equally to this work.

**Abstract:** Active granule (WC/Co<sub>3</sub>O<sub>4</sub>) doping Ti/Sb-SnO<sub>2</sub>/PbO<sub>2</sub> electrodes were successfully synthesized by composite electrodeposition. The as-prepared electrodes were systematically characterized by scanning electron microscopy (SEM), energy-dispersive X-ray spectroscopy (EDS), X-ray diffraction (XRD), X-ray photoelectron spectroscopy (XPS), electrochemical performance, zeta potential, and accelerated lifetime. It was found that the doping of active granules (WC/Co<sub>3</sub>O<sub>4</sub>) can reduce the average grain size and increase the number of active sites on the electrode surface. Moreover, it can improve the proportion of surface oxygen vacancies and non-stoichiometric PbO<sub>2</sub>, resulting in an outstanding conductivity, which can improve the electron transfer and catalytic activity of the electrode. Electrochemical measurements imply that Ti/Sb-SnO<sub>2</sub>/Co<sub>3</sub>O<sub>4</sub>-PbO<sub>2</sub> and Ti/Sb-SnO<sub>2</sub>/WC-Co<sub>3</sub>O<sub>4</sub>-PbO<sub>2</sub> electrodes have superior oxygen evolution reactions (OERs) relative to those of Ti/Sb-SnO<sub>2</sub>/PbO<sub>2</sub> and Ti/Sb-SnO<sub>2</sub>/WC-PbO<sub>2</sub> electrodes. A Ti/Sb-SnO<sub>2</sub>/Co<sub>3</sub>O<sub>4</sub>-PbO<sub>2</sub> electrode is considered as the optimal modified electrode due to its long lifetime (684 h) and the remarkable stability of plating solutions. The treatment of copper wastewater suggests that composite electrodes exhibit low cell voltage and excellent extraction efficiency. Furthermore, pilot simulation tests verified that a composite electrode consumes less energy than other electrodes. Therefore, it is inferred that composite electrodes may be promising for the treatment of wastewater containing high concentrations of copper ions.

**Keywords:** Ti/Sb-SnO<sub>2</sub>/PbO<sub>2</sub> electrode; copper-containing wastewater; active granule doping; electrocatalytic activity



**Citation:** Kang, X.; Wu, J.; Wei, Z.; Jia, B.; Feng, Q.; Xu, S.; Wang, Y.

Modification of Ti/Sb-SnO<sub>2</sub>/PbO<sub>2</sub> Electrode by Active Granules and Its Application in Wastewater Containing Copper Ions. *Catalysts*

2023, 13, 515. <https://doi.org/10.3390/catal13030515>

Academic Editors: Hao Xu and Yanbiao Liu

Received: 3 December 2022

Revised: 29 December 2022

Accepted: 30 December 2022

Published: 3 March 2023



**Copyright:** © 2023 by the authors. Licensee MDPI, Basel, Switzerland. This article is an open access article distributed under the terms and conditions of the Creative Commons Attribution (CC BY) license (<https://creativecommons.org/licenses/by/4.0/>).

## 1. Introduction

The development of the nonferrous metal industry has improved social progress and economic development. However, the nonferrous metal industry also produces many pollutants, including wastewater containing copper, zinc, nickel, etc. [1,2]. The discharge of wastewater with high concentrations of metal ions can cause serious environmental problems if it is not properly treated. The technology of metal electrodeposition from solution is environmentally friendly and has attracted considerable attention with respect to resource recovery [3–6]. For example, copper can be extracted from copper-containing wastewater by the electrochemical method, and the product can be widely used in many fields, such as light industry, electrical, national defense, etc. [7–10]. In this procedure, low oxygen evolution overpotential is favorable for energy conservation.

Electrode material is a critical component in the electrochemical process [11–13] and can affect power consumption, production cost, current efficiency, and the quality of the product. Due to the strong oxidizing ability and the corrosivity of sulfuric acid in the electrodeposition process, electrode materials (lead-based alloys, Ti-based metal oxides, Al/PbO<sub>2</sub>, and SS/PbO<sub>2</sub>) with high conductivity, good stability, mechanical strength, and

convenient processing have attracted considerable attention [14–19]. In particular, Ti-based insoluble electrode materials exhibit high corrosion resistance, long service life, excellent electrochemical performance, and electrocatalytic activity, which are highly valued with respect to environmental protection, metallurgy, and resource recovery [20–22]. Usually, Ti-based electrode material contains thinly coated noble (Ti/Ru, Ti/Ir, or Ti/Pt) electrodes and thickly coated Ti/PbO<sub>2</sub> and Ti/MnO<sub>2</sub> electrodes [23–27]. Ti/PbO<sub>2</sub> electrodes possess well-established features such as low cost, ease of synthesis, good chemical stability, and long service life, and have great application potential to copper-containing wastewater. However, the high oxygen evolution overpotential of Ti/PbO<sub>2</sub> electrodes causes energy waste during the copper electrodeposition process [28]. Reducing the oxygen evolution overpotential of the electrode is an important task for many researchers.

On the one hand, Co<sub>3</sub>O<sub>4</sub> shows superior electrocatalytic performance towards oxygen evolution reactions (OERs) due to its spinel structure, with a Co<sup>2+</sup> located in the tetrahedral site and two other Co<sup>3+</sup> atoms in the octahedral site [29–31]. On the other hand, WC can improve the mechanical properties of coatings and is widely used in the fields of cemented carbide, electrocatalytics, and fuel cells [32,33]. Therefore, in this study, active granule Co<sub>3</sub>O<sub>4</sub> and WC were introduced to Ti/Sb-SnO<sub>2</sub>/PbO<sub>2</sub> electrodes by electrodeposition with the aim of decreasing the overpotential of oxygen evolution and enhancing the service life of the electrode. An amplified simulated experiment of electrolysis was conducted to investigate the change in voltage and temperature during this process, which is closely related to energy consumption. Furthermore, wastewater containing copper ions and sulfuric acid was employed as a model recyclable resource for the electrochemical extraction of copper. The concentration of copper ions was studied by inductively coupled plasma emission spectroscopy (ICPE), and the extraction efficiency was calculated by the mass of copper deposited on the cathode.

## 2. Results and Discussion

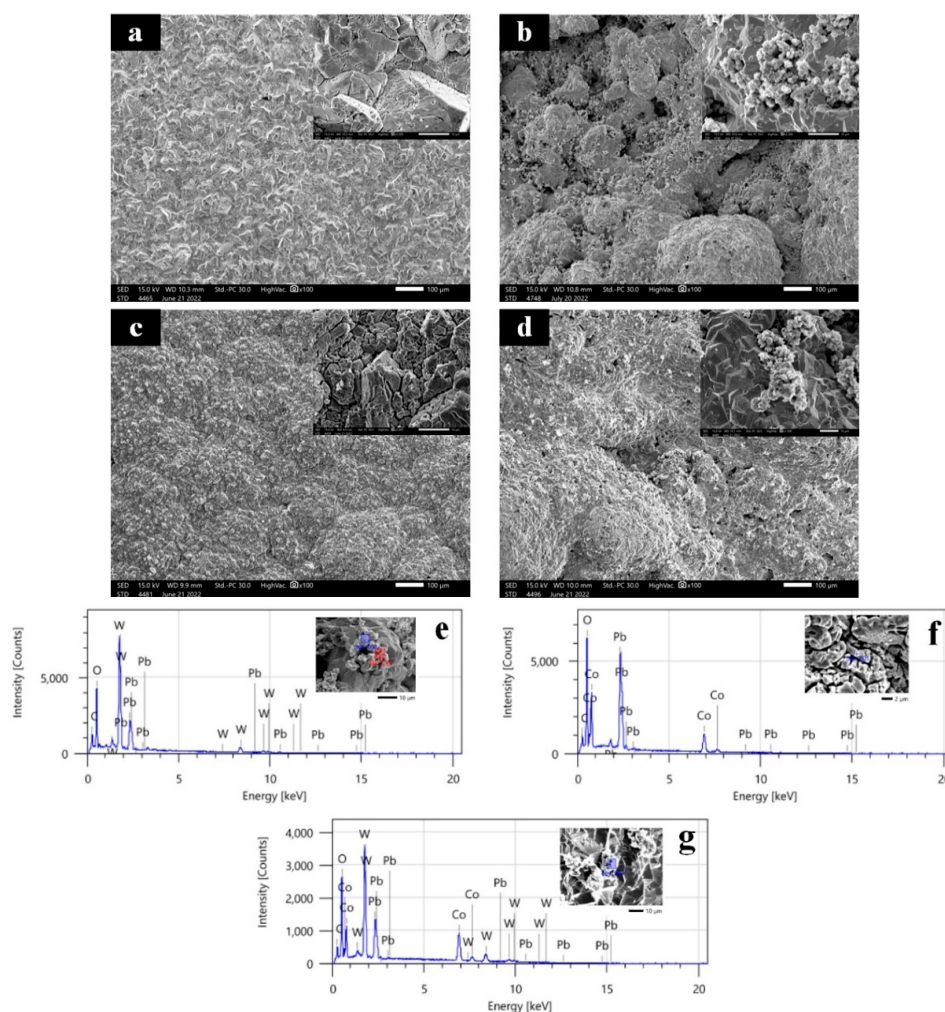
### 2.1. Surface Morphology Analysis of Electrodes

Figure 1 shows an SEM of an as-synthesized Ti/Sb-SnO<sub>2</sub>/PbO<sub>2</sub> electrode, a Ti/Sb-SnO<sub>2</sub>/WC-PbO<sub>2</sub> electrode, Ti/Sb-SnO<sub>2</sub>/Co<sub>3</sub>O<sub>4</sub>-PbO<sub>2</sub> electrode, and Ti/Sb-SnO<sub>2</sub>/WC-Co<sub>3</sub>O<sub>4</sub>-PbO<sub>2</sub> electrode. It can be seen that the Ti/Sb-SnO<sub>2</sub>/PbO<sub>2</sub> electrode shows a hill-like surface at the macroscopic level (Figure 1a). However, the hill-like surface becomes smooth after it is modified with active granules (WC/Co<sub>3</sub>O<sub>4</sub>), which indicates that the addition of active granules may affect the deposition process (Figure 1b–d). The microscopic morphology of the Ti/Sb-SnO<sub>2</sub>/PbO<sub>2</sub> electrode displays a typical tetrahedron shape. Some small particles (WC or WC-Co<sub>3</sub>O<sub>4</sub>) are agglomerated on the surface of the Ti/Sb-SnO<sub>2</sub>/WC-PbO<sub>2</sub> and Ti/Sb-SnO<sub>2</sub>/WC-Co<sub>3</sub>O<sub>4</sub>-PbO<sub>2</sub> electrodes, leading to an undulating crest of hillocks. Moreover, it was found that the surface uniformity of Ti/Sb-SnO<sub>2</sub>/Co<sub>3</sub>O<sub>4</sub>-PbO<sub>2</sub> is better than that of Ti/Sb-SnO<sub>2</sub>/WC-PbO<sub>2</sub> and Ti/Sb-SnO<sub>2</sub>/WC-Co<sub>3</sub>O<sub>4</sub>-PbO<sub>2</sub>, with a denser coating and better coverage. EDS measurements were employed to investigate the composition of particles deposited on the electrode surface (Figure 1e–g). W element was detected on the surface of the Ti/Sb-SnO<sub>2</sub>/WC-PbO<sub>2</sub> and Ti/Sb-SnO<sub>2</sub>/WC-Co<sub>3</sub>O<sub>4</sub>-PbO<sub>2</sub> electrodes. Co element was discovered on the surface of the Ti/Sb-SnO<sub>2</sub>/Co<sub>3</sub>O<sub>4</sub>-PbO<sub>2</sub> and Ti/Sb-SnO<sub>2</sub>/WC-Co<sub>3</sub>O<sub>4</sub>-PbO<sub>2</sub> electrodes. These results confirm that spherical Co<sub>3</sub>O<sub>4</sub> granules and small WC particles were successfully doped into the composite electrode.

### 2.2. XRD Structural Characterization

As shown in Figure 2, the XRD pattern of each electrode was obtained to compare the crystal structure and purity of electrodes. Figure 2 shows that bare Ti/Sb-SnO<sub>2</sub>/PbO<sub>2</sub> exhibits the reflections of  $\beta$ -PbO<sub>2</sub>. The diffraction peaks at 25.4°, 32.0°, 36.2°, 49.0°, 52.1°, 58.9°, 60.7°, and 62.5° are assigned to the (110), (101), (200), (211), (220), (310), (112), and (301) planes of  $\beta$ -PbO<sub>2</sub> (PDF#41-1492), respectively. No peaks corresponding to Sb or SnO<sub>2</sub> were detected, which can be explained by two reasons. One is the low crystallinity of the Sb-SnO<sub>2</sub> layer, and the other is the thick layer of  $\beta$ -PbO<sub>2</sub> coating on the Sb-SnO<sub>2</sub>

layer. After doping with WC particles, new peaks appeared at  $2\theta = 31.5^\circ$ ,  $35.6^\circ$ , and  $48.3^\circ$  on the Ti/Sb-SnO<sub>2</sub>/WC-PbO<sub>2</sub> electrode, which are assigned to the (001), (100), and (101) planes of WC (PDF#51-0939), respectively. However, no additional peaks were observed on Ti/Sb-SnO<sub>2</sub>/Co<sub>3</sub>O<sub>4</sub>-PbO<sub>2</sub> and Ti/Sb-SnO<sub>2</sub>/Co<sub>3</sub>O<sub>4</sub>-PbO<sub>2</sub>, which can be ascribed to the weak crystallinity, small particle size, and infinitesimal load of active particles. Moreover, the average grain sizes of Ti/Sb-SnO<sub>2</sub>/PbO<sub>2</sub>, Ti/Sb-SnO<sub>2</sub>/WC-PbO<sub>2</sub>, Ti/Sb-SnO<sub>2</sub>/Co<sub>3</sub>O<sub>4</sub>-PbO<sub>2</sub>, and Ti/Sb-SnO<sub>2</sub>/WC-Co<sub>3</sub>O<sub>4</sub>-PbO<sub>2</sub> calculated by the Debye–Scherrer equation are 56.2 nm, 38.1 nm, 48.7 nm, and 37.5 nm, respectively. The doping of active granules can decrease the grain size, which is consistent with the SEM morphology. A smaller grain size indicates more active sites on the electrode surface, which is favorable for the enhancement of catalytic performance.



**Figure 1.** SEM of the electrodes: (a) Ti/Sb-SnO<sub>2</sub>/PbO<sub>2</sub>; (b) Ti/Sb-SnO<sub>2</sub>/WC-PbO<sub>2</sub>; (c) Ti/Sb-SnO<sub>2</sub>/Co<sub>3</sub>O<sub>4</sub>-PbO<sub>2</sub>; (d) Ti/Sb-SnO<sub>2</sub>/WC-Co<sub>3</sub>O<sub>4</sub>-PbO<sub>2</sub>. EDS of the electrodes: (e) Ti/Sb-SnO<sub>2</sub>/WC-PbO<sub>2</sub>; (f) Ti/Sb-SnO<sub>2</sub>/Co<sub>3</sub>O<sub>4</sub>-PbO<sub>2</sub>; (g) Ti/Sb-SnO<sub>2</sub>/WC-Co<sub>3</sub>O<sub>4</sub>-PbO<sub>2</sub>.

### 2.3. XPS Analysis

XPS measurements were performed to further analyze the chemical state of the elements on each electrode. In the survey, the XPS spectrum of each electrode and elemental peaks for Pb and O were observed on all electrodes (Figure 3a). A new elemental peak for W and Sn was found on the Ti/Sb-SnO<sub>2</sub>/WC-PbO<sub>2</sub> electrode surface. The presence of Sn indicates that part of the coating is too thin; hence, an interlayer Sb-SnO<sub>2</sub> film was detected by XPS. This suggests that the coating on Ti/Sb-SnO<sub>2</sub>/WC-PbO<sub>2</sub> is ununiform. An additional peak for Co appeared on Ti/Sb-SnO<sub>2</sub>/Co<sub>3</sub>O<sub>4</sub>-PbO<sub>2</sub>, which confirms that

Co<sub>3</sub>O<sub>4</sub> was successfully doped in the modified PbO<sub>2</sub> film. Moreover, peaks for W and Co were found on the Ti/Sb-SnO<sub>2</sub>/WC-Co<sub>3</sub>O<sub>4</sub>-PbO<sub>2</sub> electrode, indicating the presence of WC and Co<sub>3</sub>O<sub>4</sub>. To identify the influence of active granule doping on PbO<sub>2</sub> electrodeposition, XPS analysis of Pb, O, W, and Co was performed; the results are shown in Figure 3b–e.

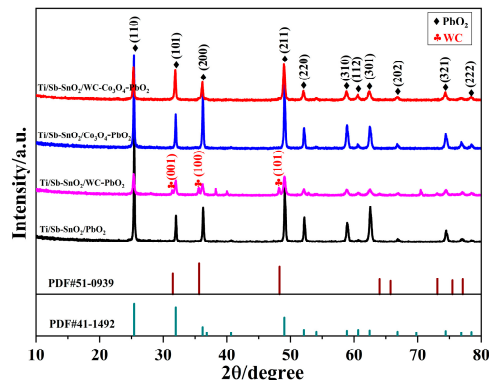


Figure 2. XRD pattern of the different samples.

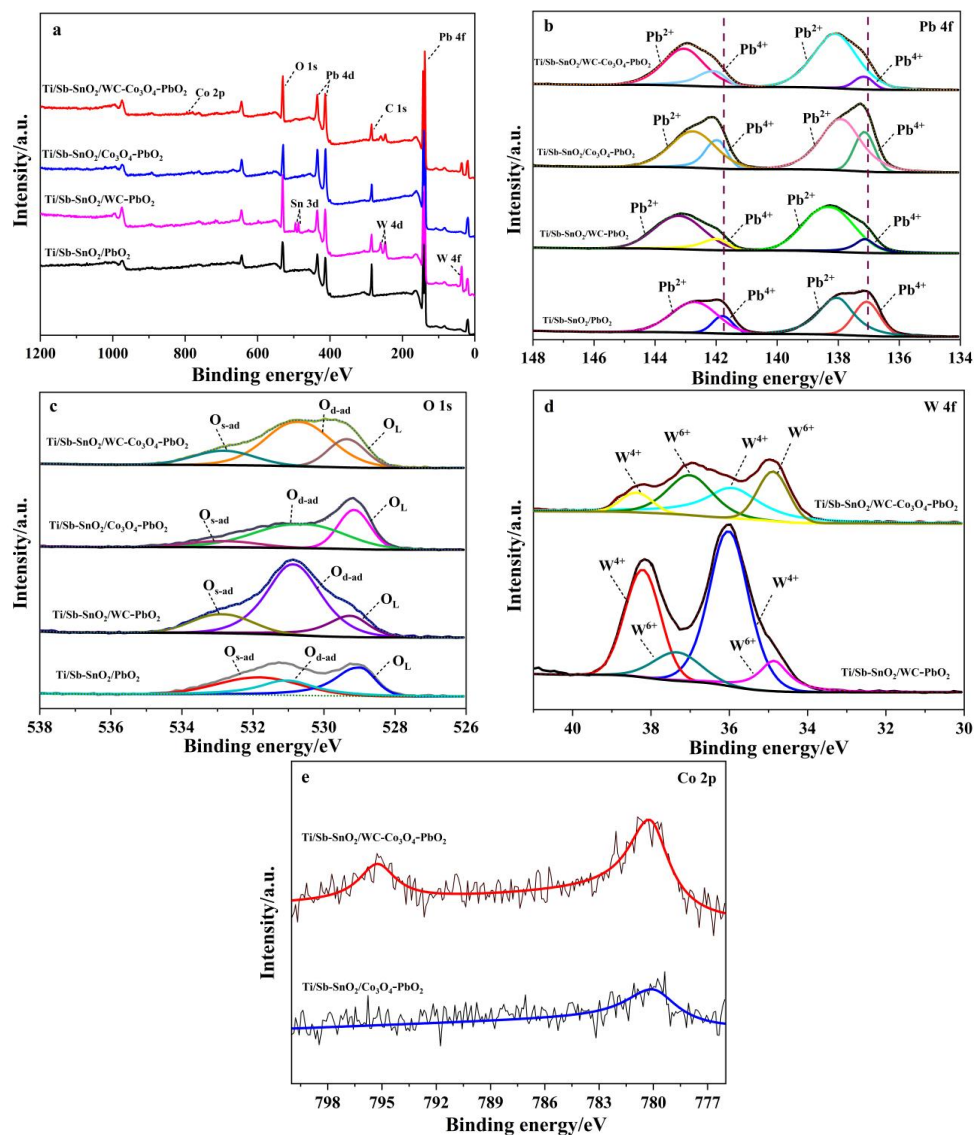


Figure 3. XPS spectra of the as-prepared samples: (a) survey, (b) Pb 4f; (c) O 1s; (d) W 4f; (e) Co 2p.

In the undoped Ti/Sb-SnO<sub>2</sub>/PbO<sub>2</sub> (Figure 3b), the binding energy peaks at 141.79 eV and 137.07 eV correspond to Pb<sup>4+</sup>, whereas the peaks at 142.70 eV and 138.02 eV are attributed to Pb<sup>2+</sup> [34], as listed in Table 1. Moreover, the simultaneous presence of Pb<sup>4+</sup> and Pb<sup>2+</sup> in the PbO<sub>2</sub> coating implies the formation of non-stoichiometric PbO<sub>2</sub> during the electrodeposition process. After doping with active granules, the peaks of Pb<sup>4+</sup> on modified electrodes shifted to the higher binding energy, which suggests that active granules have a strong interaction with Pb. The proportion of Pb<sup>4+</sup> in Ti/Sb-SnO<sub>2</sub>/PbO<sub>2</sub>, Ti/Sb-SnO<sub>2</sub>/WC-PbO<sub>2</sub>, Ti/Sb-SnO<sub>2</sub>/Co<sub>3</sub>O<sub>4</sub>-PbO<sub>2</sub>, and Ti/Sb-SnO<sub>2</sub>/WC-Co<sub>3</sub>O<sub>4</sub>-PbO<sub>2</sub> is 29.9%, 15.9%, 27.12%, and 15.61%, respectively. The decrease in Pb<sup>4+</sup> after modification with active granules implies that part of the PbO<sub>2</sub> converts to lower-valence compounds, enhancing the non-stoichiometric PbO<sub>2</sub>, which could improve the conductivity of the electrode.

**Table 1.** The binding energy of Pb 4f on each electrode.

Electrode	Pb <sup>4+</sup> 4f <sub>7/2</sub> /eV	Pb <sup>4+</sup> 4f <sub>5/2</sub> /eV	Pb <sup>2+</sup> 4f <sub>7/2</sub> /eV	Pb <sup>2+</sup> 4f <sub>5/2</sub> /eV
Ti/Sb-SnO <sub>2</sub> /PbO <sub>2</sub>	137.07	141.79	138.02	142.70
Ti/Sb-SnO <sub>2</sub> /WC-PbO <sub>2</sub>	137.12	141.94	138.26	143.22
Ti/Sb-SnO <sub>2</sub> /Co <sub>3</sub> O <sub>4</sub> -PbO <sub>2</sub>	137.14	141.95	137.89	142.76
Ti/Sb-SnO <sub>2</sub> /WC-Co <sub>3</sub> O <sub>4</sub> -PbO <sub>2</sub>	137.13	142.05	138.10	143.05

The O 1s core level shown in Figure 3c can be deconvoluted into four characteristic peaks of lattice oxygen species (528.9–530.4 eV for O<sub>L</sub>), surface oxygen vacancies, adsorbed oxygen (530.5–531.7 eV for O<sub>d-ad</sub>), and surface-adsorbed oxygen species (531.8–532.8 eV for O<sub>s-ad</sub>), as listed in Table 2. According to the literature [35], the formation of surface oxygen vacancies is closely related to highly oxidative oxygen species and is active for catalysis of OER. The proportions of O<sub>d-ad</sub> present on the electrode surface significantly increase after decoration with active granules, which is beneficial to the OER activity.

**Table 2.** The binding energy of O 1s and its proportions on each electrode.

Electrode	O <sub>L</sub> /eV	O <sub>L</sub> /%	O <sub>d-ad</sub> /eV	O <sub>d-ad</sub> /%	O <sub>s-ad</sub> /eV	O <sub>s-ad</sub> /%
Ti/Sb-SnO <sub>2</sub> /PbO <sub>2</sub>	529.01	27.69%	531.01	20.91%	531.82	29.56%
Ti/Sb-SnO <sub>2</sub> /WC-PbO <sub>2</sub>	529.25	17.06%	530.84	64.53%	532.83	18.41%
Ti/Sb-SnO <sub>2</sub> /Co <sub>3</sub> O <sub>4</sub> -PbO <sub>2</sub>	529.15	34.53%	530.55	54.72%	532.77	10.75%
Ti/Sb-SnO <sub>2</sub> /WC-Co <sub>3</sub> O <sub>4</sub> -PbO <sub>2</sub>	529.35	21.16%	530.67	59.91%	532.81	18.93%

Figure 3d shows the W 4f spectrum; the binding energy peaks at 35.96 eV and 38.29 eV are assigned to W<sup>4+</sup>, whereas the peaks at 34.87 eV and 37.17 eV are ascribed to W<sup>6+</sup>. This consequence demonstrates the generation of WC. However, W<sup>6+</sup> also appears on the electrode surface. The formation of W<sup>6+</sup> can be attributed to the oxidation of WC during composite electrodeposition. Moreover, the XPS spectrum of Co 2p is very weak due to the extremely limited doping of active particles. It was found that two main peaks appeared on the Ti/Sb-SnO<sub>2</sub>/WC-Co<sub>3</sub>O<sub>4</sub>-PbO<sub>2</sub> electrode. The peaks located at 795.26 eV and 780.23 eV are identical to Co 2p<sub>1/2</sub> and Co 2p<sub>3/2</sub>, respectively (Figure 3e), which confirms the presence of Co<sub>3</sub>O<sub>4</sub>.

#### 2.4. Electrochemical Properties

LSV measurements of the as-prepared samples were performed on an electrochemical workstation to investigate the OER performance of the electrodes. The onset potential for oxygen evolution potential (OEP) on Ti/Sb-SnO<sub>2</sub>/PbO<sub>2</sub>, Ti/Sb-SnO<sub>2</sub>/WC-PbO<sub>2</sub>, Ti/Sb-SnO<sub>2</sub>/Co<sub>3</sub>O<sub>4</sub>-PbO<sub>2</sub>, and Ti/Sb-SnO<sub>2</sub>/WC-Co<sub>3</sub>O<sub>4</sub>-PbO<sub>2</sub> is 2.20 V, 2.12 V, 1.85 V, and 1.80 V (vs. Ag/AgCl), respectively. A low OER means that oxygen is more easily formed during the electrochemical process. Therefore, it is speculated that the modification of active granules (WC/Co<sub>3</sub>O<sub>4</sub>) can improve the OER properties of electrodes due to the presence of more active sites and increased electrocatalytic activity. Moreover, doping with Co<sub>3</sub>O<sub>4</sub> is more efficient than doping with WC. This can be attributed to the special properties of Co<sub>3</sub>O<sub>4</sub> and its better OER performance. Furthermore, the non-uniformity of the WC-PbO<sub>2</sub> coating

may enhance resistance, hindering the formation of oxygen. As shown in the illustration in Figure 4, when the current density is  $200 \text{ A/m}^2$ , the potential of Ti/Sb-SnO<sub>2</sub>/PbO<sub>2</sub>, Ti/Sb-SnO<sub>2</sub>/WC-PbO<sub>2</sub>, Ti/Sb-SnO<sub>2</sub>/Co<sub>3</sub>O<sub>4</sub>-PbO<sub>2</sub>, and Ti/Sb-SnO<sub>2</sub>/WC-Co<sub>3</sub>O<sub>4</sub>-PbO<sub>2</sub> is 2.14 V, 1.96 V, 1.88 V, and 1.75 V (vs. Ag/AgCl), respectively. This implies that Ti/Sb-SnO<sub>2</sub>/Co<sub>3</sub>O<sub>4</sub>-PbO<sub>2</sub> and Ti/Sb-SnO<sub>2</sub>/WC-Co<sub>3</sub>O<sub>4</sub>-PbO<sub>2</sub> need lower potential than Ti/Sb-SnO<sub>2</sub>/PbO<sub>2</sub> and Ti/Sb-SnO<sub>2</sub>/WC-PbO<sub>2</sub> under the same current density. Low potential is more helpful for saving energy during electrolysis.

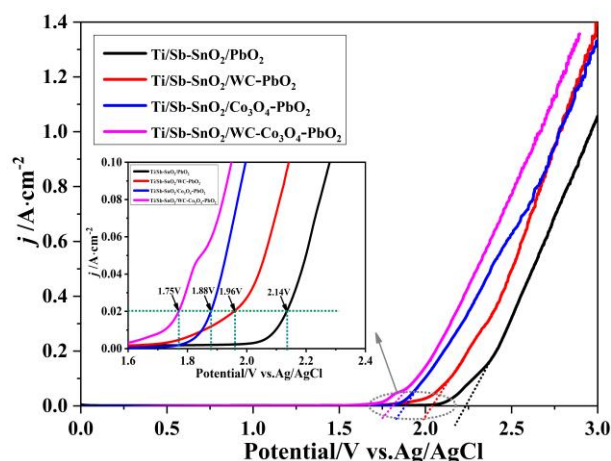


Figure 4. LSV curves of the different electrodes.

Energy conservation has become an important problem due to energy shortages. As is known to all, voltage is closely related to energy consumption. How to reduce the voltage of electrolysis is a crucial issue in the electrolytic industry. Therefore, a simulation experiment of electrolysis under a current density of  $200 \text{ A/m}^2$  was conducted to explore the variation in voltage, as displayed in Figure 5. It was found that the Ti/Sb-SnO<sub>2</sub>/Co<sub>3</sub>O<sub>4</sub>-PbO<sub>2</sub> and Ti/Sb-SnO<sub>2</sub>/WC-Co<sub>3</sub>O<sub>4</sub>-PbO<sub>2</sub> electrodes have advantages over the Ti/Sb-SnO<sub>2</sub>/PbO<sub>2</sub> and Ti/Sb-SnO<sub>2</sub>/WC-PbO<sub>2</sub> electrodes. These results are consistent with the LSV measurements.

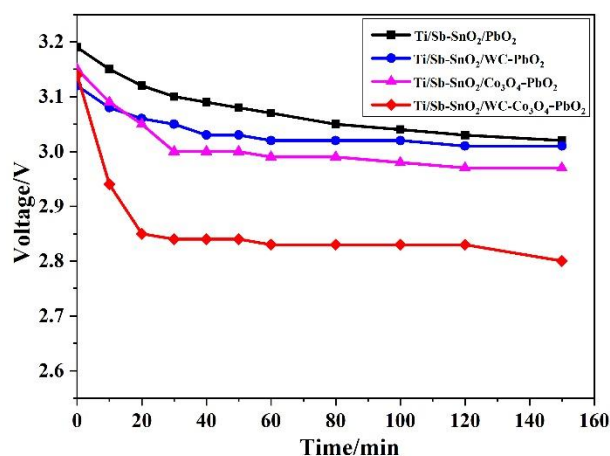
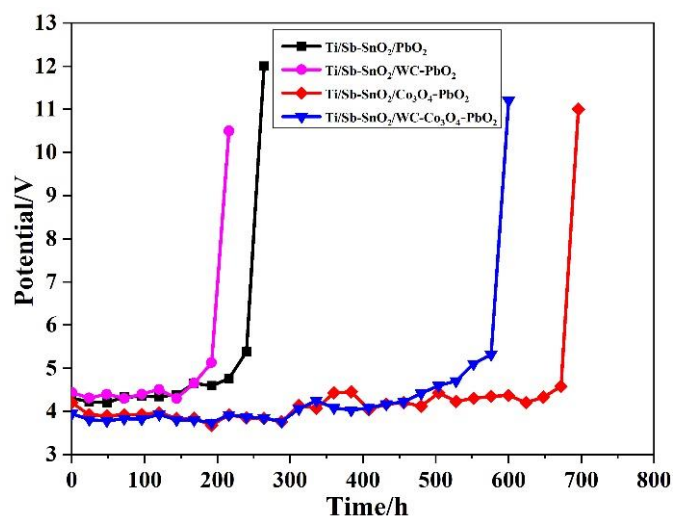


Figure 5. The change in voltage during electrolysis ( $200 \text{ A/m}^2$ ; 15% H<sub>2</sub>SO<sub>4</sub> aqueous solutions).

Moreover, an accelerated life test was carried out to evaluate the electrochemical stability of the electrodes. Figure 6 shows the time course of cell potential in the accelerated life test. It was observed that the Ti/Sb-SnO<sub>2</sub>/PbO<sub>2</sub>, Ti/Sb-SnO<sub>2</sub>/WC-PbO<sub>2</sub>, Ti/Sb-SnO<sub>2</sub>/Co<sub>3</sub>O<sub>4</sub>-PbO<sub>2</sub>, and Ti/Sb-SnO<sub>2</sub>/WC-Co<sub>3</sub>O<sub>4</sub>-PbO<sub>2</sub> electrodes exhibited a lifetime of 252 h, 204 h, 684 h, and 592 h, respectively. The lifetime of Ti/Sb-SnO<sub>2</sub>/WC-PbO<sub>2</sub> is shorter than that of Ti/Sb-SnO<sub>2</sub>/PbO<sub>2</sub>, which can be attributed to the non-uniformity of its

coating. The lifetimes of Ti/Sb-SnO<sub>2</sub>/Co<sub>3</sub>O<sub>4</sub>-PbO<sub>2</sub> and Ti/Sb-SnO<sub>2</sub>/WC-Co<sub>3</sub>O<sub>4</sub>-PbO<sub>2</sub> are increased by more than two-fold relative to that of Ti/Sb-SnO<sub>2</sub>/PbO<sub>2</sub>.



**Figure 6.** Variation of the cell potential with testing time in an accelerated life test for the as-synthesized samples (10,000 A/m<sup>2</sup>; 15% H<sub>2</sub>SO<sub>4</sub> aqueous solutions).

### 2.5. The Application of Modified Electrodes in Wastewater Containing Copper Ions

Deposition solutions containing active granules (WC/Co<sub>3</sub>O<sub>4</sub>) were tested with a zeta potential analyzer to study their stability [36]. The Zeta potential of deposition solutions with WC, Co<sub>3</sub>O<sub>4</sub>, and WC-Co<sub>3</sub>O<sub>4</sub> are 3.9 mV, 5.5 mV, and 3.4 mV, respectively. It was found that a high absolute value of zeta potential indicates higher stability against coagulation, which implies excellent stability in such systems. Compared to other deposition systems, the plating solution with Co<sub>3</sub>O<sub>4</sub> exhibits the best stability. Although Ti/Sb-SnO<sub>2</sub>/WC-Co<sub>3</sub>O<sub>4</sub>-PbO<sub>2</sub> shows the lowest OER property, the stability of the plating solution with WC-Co<sub>3</sub>O<sub>4</sub> is the worst. Therefore, considering the lifetime of the electrode and the stability of the solution, we selected the Ti/Sb-SnO<sub>2</sub>/Co<sub>3</sub>O<sub>4</sub>-PbO<sub>2</sub> electrode as the optimal electrode for subsequent experiments.

Electrochemical extraction experiments were carried out to investigate the application of electrodes to wastewater containing copper ions. This system contains two Ti/Sb-SnO<sub>2</sub>/Co<sub>3</sub>O<sub>4</sub>-PbO<sub>2</sub> anodes and one SS cathode with magnetic stirring. As shown in Figure 7a, the color of copper deposited on the electrode becomes dark due to the ion impoverishment of copper ions. Usually, dark copper is generated when the copper ion concentration decreases to a certain value in actual production. Figure 7b displays the mass and concentration of copper over time; the mass of copper increases linearly with time, and the concentration of copper ions decreases with time. The Ti/Sb-SnO<sub>2</sub>/Co<sub>3</sub>O<sub>4</sub>-PbO<sub>2</sub> electrode shows a higher mass and a lower concentration than the Ti/Sb-SnO<sub>2</sub>/PbO<sub>2</sub> electrode. The extraction efficiency of Ti/Sb-SnO<sub>2</sub>/Co<sub>3</sub>O<sub>4</sub>-PbO<sub>2</sub> and Ti/Sb-SnO<sub>2</sub>/PbO<sub>2</sub> is 99.1% and 83.2%, respectively (Figure 7c). Moreover, the cell voltage of Ti/Sb-SnO<sub>2</sub>/Co<sub>3</sub>O<sub>4</sub>-PbO<sub>2</sub> is lower than that of Ti/Sb-SnO<sub>2</sub>/PbO<sub>2</sub>, indicating less energy consumption (Figure 7d). These results reveal that the modified Ti/Sb-SnO<sub>2</sub>/Co<sub>3</sub>O<sub>4</sub>-PbO<sub>2</sub> electrode has superior performance in the extraction of copper from wastewater by the electrochemical method.

Laboratory experiments usually slightly deviate from actual working conditions. Therefore, we decided to build a magnifying system that is close to practical working conditions. To that end, an apparatus was manufactured and outsourcing factory consisting of a circular aeration, heat, and electric control (Figure 8a). Amplification tests were performed to research the energy consumption of this device. To simplify the experimental process, we employed 15% H<sub>2</sub>SO<sub>4</sub> aqueous solutions to simulate acidic working conditions. The other parameters were similar to those used in the electrochemical extraction experiment. In the pilot simulation tests, the Ti/Sb-SnO<sub>2</sub>/Co<sub>3</sub>O<sub>4</sub>-PbO<sub>2</sub>, Ti/Sb-SnO<sub>2</sub>/PbO<sub>2</sub>, and Pb electrodes were employed as the anode, and SS was used as the cathode, all with dimensions of

200 mm × 290 mm × 4 mm (Figure 8b). It should be noted that Pb electrodes are traditionally used in the metallurgical industry. Ti/Sb-SnO<sub>2</sub>/Co<sub>3</sub>O<sub>4</sub>-PbO<sub>2</sub> had a lower voltage and lower temperature (Figure 8c,d) than Ti/Sb-SnO<sub>2</sub>/PbO<sub>2</sub> and Pb. These results suggest that Ti/Sb-SnO<sub>2</sub>/Co<sub>3</sub>O<sub>4</sub>-PbO<sub>2</sub> consumes less energy than Ti/Sb-SnO<sub>2</sub>/PbO<sub>2</sub> and Pb electrodes, which is in agreement with the results of the electrochemical extraction experiments. This indicates that Ti/Sb-SnO<sub>2</sub>/Co<sub>3</sub>O<sub>4</sub>-PbO<sub>2</sub> electrodes may replace traditional Pb electrodes in the resource recovery of nonferrous metals.

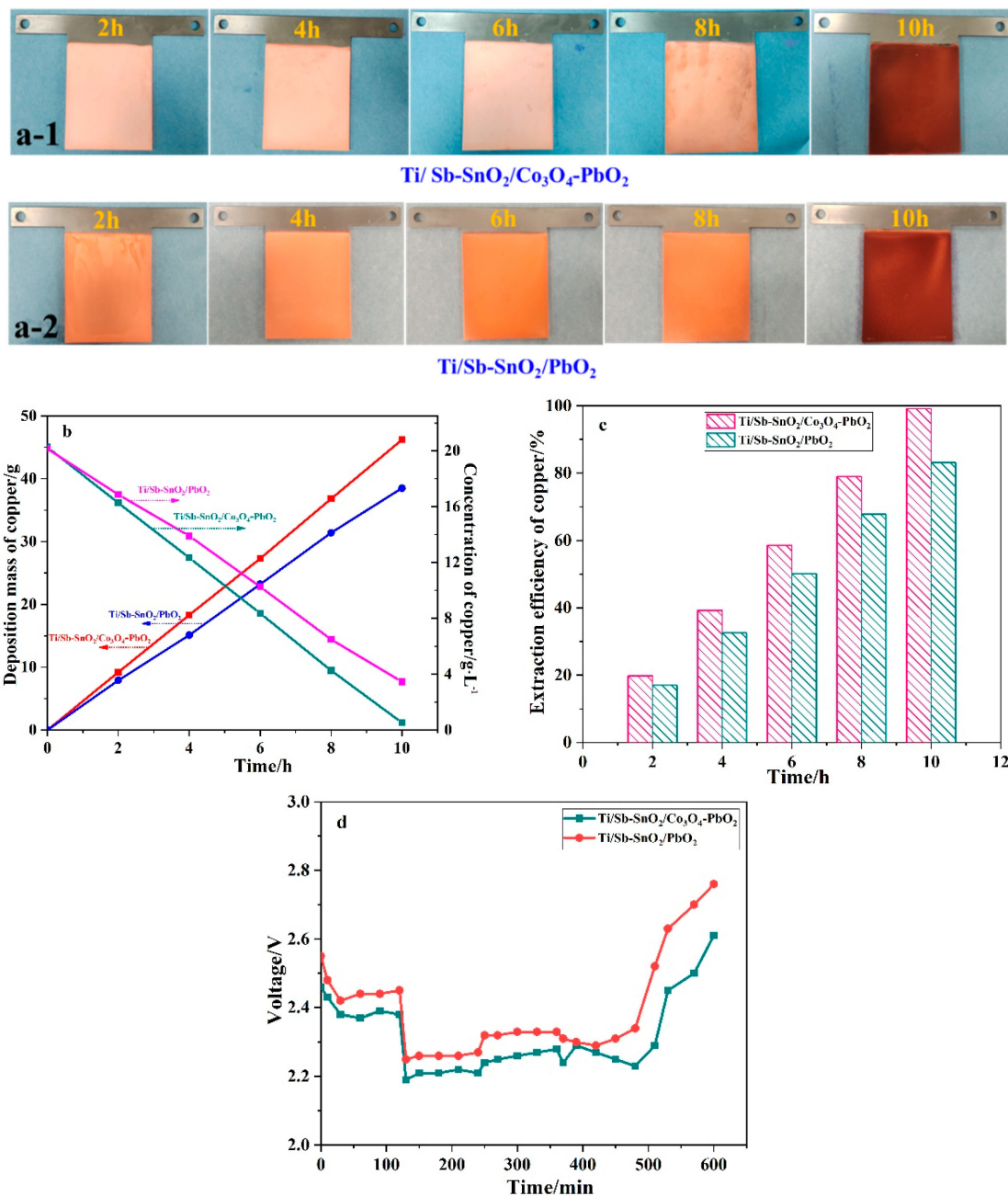


**Figure 7.** (a) Digital images of copper deposited on Ti/Sb-SnO<sub>2</sub>/Co<sub>3</sub>O<sub>4</sub>-PbO<sub>2</sub> (a-1) and Ti/Sb-SnO<sub>2</sub>/PbO<sub>2</sub> (a-2) at different times. (b) Variation in the deposition mass and concentration of copper over time. (c) The extraction efficiency of copper during the electrochemical process. (d) The cell voltage of different electrodes during electrodeposition.



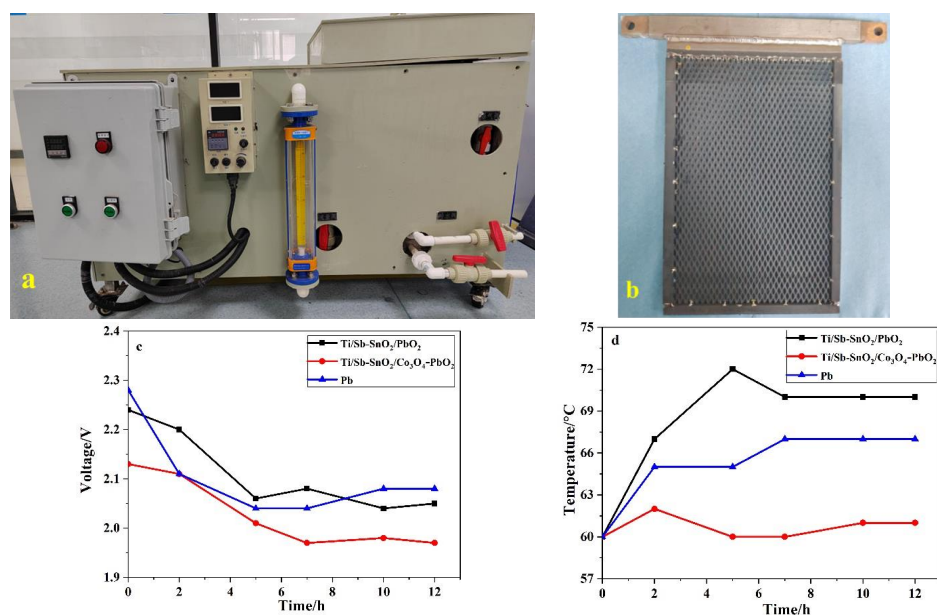


**Figure 8.** (a) Pilot apparatus of the simulation test. (b) Part of the sample used in the pilot test. (c) The variation in cell voltage during the electrochemical process. (d) The change in temperature during the electrochemical process.

### 3. Experimental Details

#### 3.1. Materials

All chemicals were of analytical grade and were used without any further purification. SnCl<sub>2</sub>·2H<sub>2</sub>O and SbCl<sub>3</sub> were provided by Xilong Scientific Co., Ltd. (Chaoshan, China). Ethanol and tert-butyl alcohol were offered by Tianjin Fuyu Fine Chemical Co., Ltd. (Tianjin, China). Pb(NO<sub>3</sub>)<sub>2</sub>, Cu(NO<sub>3</sub>)<sub>2</sub>, NaF, and some additives were obtained from Sinopharm Chemical Reagent Co., Ltd. (Shanghai, China). HNO<sub>3</sub>, H<sub>2</sub>SO<sub>4</sub>, and HCl were produced from Xi'an Sanpu Chemical Reagents Co., Ltd. (Xi'an, China). WC and Co<sub>3</sub>O<sub>4</sub> reagents were purchased from MACKLIN (Shanghai, China). All solutions were prepared with deionized water (DI). Titanium foil (Baoji Baite Metal Co., Ltd., Baoji, China, 1.5 mm thickness) was cut into pieces with effective dimensions of 80 mm × 100 mm before experiments.

#### 3.2. Fabrication of Ti/Sb-SnO<sub>2</sub>/PbO<sub>2</sub> Electrode by Active Granules

A Ti sheet was subjected to pretreatment before the experiment, including polishing, degreasing, and etching in boiling oxalic acid for 2 h, to obtain a gray surface with uniform roughness. Sb-SnO<sub>2</sub> was introduced as a conductive transition layer between the PbO<sub>2</sub> film layer and the Ti substrate by the thermal decomposition approach. Sb-SnO<sub>2</sub> precursor solutions were prepared by dissolving a SnCl<sub>4</sub> and SbCl<sub>3</sub> mixture in a mixed solvent at a molar ratio of 10:1. The coating liquids were evenly brushed on the Ti sheet. Then, the Ti sheet was dried at 100 °C and annealed at 450 °C. The brushing, drying, and calcining steps were repeated several times.

PbO<sub>2</sub> coatings with active granules (Co<sub>3</sub>O<sub>4</sub> and WC) were synthesized by composite electrodeposition with a current density of 200 A/m<sup>2</sup> for 2 h at 60 °C. The deposition solutions containing Pb(NO<sub>3</sub>)<sub>2</sub>, Cu(NO<sub>3</sub>)<sub>2</sub>, HNO<sub>3</sub>, active granules (WC/Co<sub>3</sub>O<sub>4</sub>), and other additives were ultrasonicated for 30 min. The as-prepared electrodes were rinsed thoroughly with DI and are denoted as Ti/Sb-SnO<sub>2</sub>/PbO<sub>2</sub>, Ti/Sb-SnO<sub>2</sub>/WC-PbO<sub>2</sub>, Ti/Sb-SnO<sub>2</sub>/Co<sub>3</sub>O<sub>4</sub>-PbO<sub>2</sub>, and Ti/Sb-SnO<sub>2</sub>/WC-Co<sub>3</sub>O<sub>4</sub>-PbO<sub>2</sub>.

#### 3.3. Characterization

A scanning electron microscope (SEM, JSM-IT200, JEOL, Tokyo, Japan) equipped with an energy-dispersive X-ray spectroscopy (EDS, JEOL) detector was employed to study the surface morphology and composition of the as-prepared samples. X-ray diffraction (XRD,

D8 Advance, Bruker, Karlsruhe, Germany) measurement was conducted on an X'pert PRO MRD diffractometer using a Cu-K $\alpha$  source ( $\lambda = 0.15416$  nm) with a scanning angle ( $2\theta$ ) range of  $10\text{--}80^\circ$ . Chemical states of Pb, O, W, and Co in the composite electrodes were identified by X-ray photoelectron spectroscopy (XPS, ESCALAB 250Xi, Thermo Fisher Scientific, Waltham, MA, USA) on an Ultra DLD Electron Spectrometer (Al K $\alpha$  radiation;  $h\nu = 1486.71$  eV). XPS data were calibrated using the binding energy of C1s (284.8 eV) as the standard and were fitted using commercial software (Thermo Avantage). The zeta potential of the deposition solutions containing active granules (WC/Co $_3$ O $_4$ ) was tested on a zeta potential analyzer (Stabino zeta, Microtrac MRB, Dusseldorf, Germany) to study the stability of the solutions.

Electrochemical performance was evaluated on an electrochemical workstation (Corrtest CS2350, Corrtest Instruments Corp., Ltd., Wuhan, China) using the traditional three-electrode system. A Pt sheet is used as counter electrode, a saturated Ag/AgCl electrode is employed as reference electrode, and the as-prepared electrode served as working electrode. Linear sweep voltammetric (LSV) characterization was measured in 15% H $_2$ SO $_4$  aqueous solutions at a scan rate of 10 mV/s. simulated electrochemical experiment is also tested in 15% H $_2$ SO $_4$  aqueous solutions to study the change in voltage during electrolysis. Accelerated life tests were carried out to research the stability and lifetime of the as-prepared electrodes in 15% H $_2$ SO $_4$  aqueous solutions with a current density of 10,000 A/m $^2$ . In this procedure, the experiment was considered finished when the cell voltage exceeded 10 V.

### 3.4. Electrochemical Treatment of Copper-Containing Wastewater

Wastewater containing copper ions was treated by electrochemical approaches in a large beaker equipped with a water bath and magnetic stirrer, as shown in Figure 9. Two pieces of Ti/Sb-SnO $_2$ /Co $_3$ O $_4$ -PbO $_2$  electrodes were used as the anode, and stainless steel (SS) was employed as the cathode. The temperature was set to 60 °C, and the current density was set to 200 A/m $^2$ . Simulated wastewater with a high concentration of copper ions (20 g/L Cu $^{2+}$ ) was prepared by dissolving CuSO $_4$ ·5H $_2$ O in 15% H $_2$ SO $_4$  aqueous solutions. During experiments, samples were taken out of the beaker every 2 h for ICPE measurement, and the SS cathode was weighed every 2 h to calculate the mass of copper deposited on the cathode. The variation in cell voltage during this chemical process was also recorded to compare the energy consumption. The extraction efficiency of copper was calculated as follows:

$$\text{Extraction efficiency}/\% = \frac{m_0 - m_t}{m_0} \times 100\% = \frac{C_0 \times V - m_t}{C_0 \times V} \times 100\% \quad (1)$$

where  $m_0$  and  $m_t$  are the mass of copper before and after an electrolysis time of  $t$ , respectively;  $C_0$  is the initial concentration of copper ions, which can be obtained by the ICPE technique; and  $V$  is the volume of the solutions.

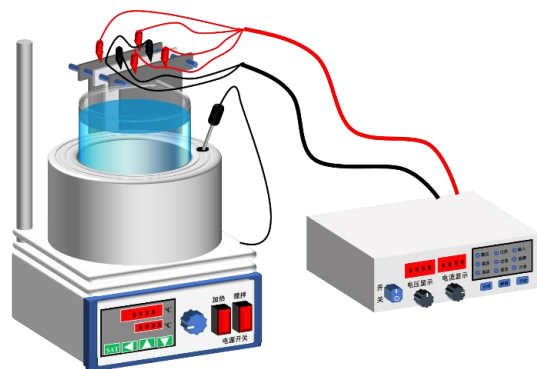


Figure 9. Schematic diagram of treatment of wastewater containing copper ions.

#### 4. Conclusions

In summary, active granule (WC/Co<sub>3</sub>O<sub>4</sub>) modified Ti/Sb-SnO<sub>2</sub>/PbO<sub>2</sub> electrodes were fabricated by composite electrodeposition. EDS and XPS characterization of the as-prepared electrodes suggests that active granules (WC/Co<sub>3</sub>O<sub>4</sub>) were successfully deposited on the surface of Ti/Sb-SnO<sub>2</sub>/WC-PbO<sub>2</sub>, Ti/Sb-SnO<sub>2</sub>/Co<sub>3</sub>O<sub>4</sub>-PbO<sub>2</sub>, and Ti/Sb-SnO<sub>2</sub>/WC-Co<sub>3</sub>O<sub>4</sub>-PbO<sub>2</sub> composite electrodes. The introduction of active granules (WC/Co<sub>3</sub>O<sub>4</sub>) can decrease the average grain size and enhance the proportions of O<sub>d-ad</sub> present on the electrode surface, leading to more active sites on the electrode surface. Moreover, the excellent conductivity of the electrode caused by the presence of non-stoichiometric PbO<sub>2</sub> was also observed, which is favorable for improving the electron transfer and catalytic activity of the electrode. LSV measurements show that Ti/Sb-SnO<sub>2</sub>/Co<sub>3</sub>O<sub>4</sub>-PbO<sub>2</sub> (1.85 V) and Ti/Sb-SnO<sub>2</sub>/WC-Co<sub>3</sub>O<sub>4</sub>-PbO<sub>2</sub> (1.80 V) have lower OER values than Ti/Sb-SnO<sub>2</sub>/PbO<sub>2</sub> (2.20 V) and Ti/Sb-SnO<sub>2</sub>/WC-PbO<sub>2</sub> (2.12 V). Ti/Sb-SnO<sub>2</sub>/Co<sub>3</sub>O<sub>4</sub>-PbO<sub>2</sub> is regarded as the optimal modified electrode due to its long service lifetime (684 h) and the good stability of its plating solutions. Wastewater containing copper ions was employed as a model pollutant, and Ti/Sb-SnO<sub>2</sub>/Co<sub>3</sub>O<sub>4</sub>-PbO<sub>2</sub> was used as the anode to study the electrocatalytic activity of the modified electrodes. The experimental results demonstrate that the Ti/Sb-SnO<sub>2</sub>/Co<sub>3</sub>O<sub>4</sub>-PbO<sub>2</sub> composite electrode exhibits remarkable extraction efficiency and low cell voltage. The color of copper deposited on the cathode became dark due to the impoverishment of copper ions. Furthermore, pilot simulation tests were carried out to research the electrodes in practical applications. A low cell voltage further verified that the composite electrodes consume less energy than other electrodes. Therefore, it is deduced that composite electrodes may be promising for the treatment of wastewater containing high concentrations of copper ions. Furthermore, it is expected that Ti/Sb-SnO<sub>2</sub>/Co<sub>3</sub>O<sub>4</sub>-PbO<sub>2</sub> electrodes may substitute traditional Pb electrodes in resource recovery of nonferrous metals. Further studies exploring modified electrodes in specific pilot tests will be conducted in the future.

**Author Contributions:** Conceptualization, X.K. and S.X.; Methodology, X.K. and B.J.; Software, Q.F.; Validation, X.K., J.W., Z.W. and S.X.; Formal analysis, X.K., J.W. and Z.W.; Investigation, X.K. and Z.W.; Resources, X.K. and Q.F.; Data curation, J.W.; Writing—original draft, J.W.; Writing—review and editing, Y.W.; Supervision, X.K. and Q.F.; Project administration, B.J.; Funding acquisition, Y.W. All authors have read and agreed to the published version of the manuscript.

**Funding:** The authors gratefully acknowledge the financial support from the National Natural Science Foundation of China (Grant No. 21878242).

**Data Availability Statement:** All data supporting this study are available from authors upon request.

**Acknowledgments:** The Northwest Institute for Non-ferrous Metal Research is acknowledged.

**Conflicts of Interest:** The authors declare no conflict of interest.

#### References

1. Lin, B.; Zhang, G. Estimates of electricity saving potential in chinese nonferrous metals industry. *Energy Policy* **2013**, *60*, 558–568. [[CrossRef](#)]
2. Yang, Y.; Yang, L.; Wang, M.; Yang, Q.; Liu, X.; Shen, J.; Liu, G.; Zheng, M. Concentrations and profiles of persistent organic pollutants unintentionally produced by secondary nonferrous metal smelters: Updated emission factors and diagnostic ratios for identifying sources. *Chemosphere* **2020**, *255*, 126958. [[CrossRef](#)]
3. Sorour, N.; Zhang, W.; Gabra, G.; Ghali, E.; Houlachi, G. Electrochemical studies of ionic liquid additives during the zinc electrowinning process. *Hydrometallurgy* **2015**, *157*, 261–269. [[CrossRef](#)]
4. Zhang, C.; Duan, N.; Jiang, L.; Xu, F. The impact mechanism of Mn<sup>2+</sup> ions on oxygen evolution reaction in zinc sulfate electrolyte. *J. Electroanal. Chem.* **2018**, *811*, 53–61. [[CrossRef](#)]
5. Karbasi, M.; Eskandar, K.A.; Elaheh, A.D. Electrochemical performance of Pb–Co composite anode during zinc electrowinning. *Hydrometallurgy* **2018**, *183*, 51–59. [[CrossRef](#)]
6. Chen, B.; Wang, S.; Liu, J.; Huang, H.; Dong, C.; He, Y.; Yan, W.; Guo, Z.; Xu, R.; Yang, H. Corrosion resistance mechanism of a novel porous Ti/Sn-Sb-RuO<sub>x</sub>/β-PbO<sub>2</sub> anode for zinc electrowinning. *Corros. Sci.* **2018**, *144*, 136–144. [[CrossRef](#)]
7. Zhang, H.; Chen, J.; Ni, S.; Bie, C.; Zhi, H.; Sun, X. A clean process for selective recovery of copper from industrial wastewater by extraction-precipitation with p-tert-octyl phenoxy acetic acid. *J. Environ. Manag.* **2022**, *304*, 114164. [[CrossRef](#)]

8. Zhang, L.; Lu, Z.; Chen, P. An environmentally friendly gradient treatment system of copper-containing wastewater by coupling thermally regenerative battery and electrodeposition cell. *Sep. Purif. Technol.* **2022**, *295*, 121243. [[CrossRef](#)]
9. Zhang, X.; Zhang, S. Enhanced copper extraction in the chalcopyrite bioleaching system assisted by microbial fuel cells and catalyzed by silver-bearing ores. *J. Environ. Chem. Eng.* **2022**, *10*, 108827. [[CrossRef](#)]
10. Zhou, W.; Liu, X.; Lyu, X.; Gao, W.; Su, H.; Li, C. Extraction and separation of copper and iron from copper smelting slag: A review. *J. Clean. Prod.* **2022**, *368*, 133095. [[CrossRef](#)]
11. Kim, H.K.; Jang, H.; Jin, X.; Kim, M.G.; Hwang, S.J. A crucial role of enhanced Volmer-Tafel mechanism in improving the electrocatalytic activity via synergetic optimization of host, interlayer, and surface features of 2D nanosheets. *Appl. Catal. B Environ.* **2022**, *312*, 121391. [[CrossRef](#)]
12. Abedini, A.; Valmoozi, A.A.E.; Afghahi, S.S.S. Anodized graphite as an advanced substrate for electrodeposition of PbO<sub>2</sub>. *Mater. Today Commun.* **2022**, *31*, 103464. [[CrossRef](#)]
13. Kandasamy, K. Electrochemical degradation of sago wastewater using Ti/PbO<sub>2</sub> electrode: Optimisation using response surface methodology. *Int. J. Electrochem. Sci.* **2014**, *10*, 1506–1516.
14. Torres, J.E.; Sierra, A.; Pena, D.Y.; Uribe, I.; Estupinan, H. Corrosion rate in a lead based alloy in a sulfuric acid solution at different temperatures. *Matéria* **2014**, *19*, 183–196.
15. Li, H.; Yuan, T.; Li, R.; Wang, W.; Zheng, D.; Yuan, J. Electrochemical properties of powder-pressed Pb-Ag-PbO<sub>2</sub> anodes. *Trans. Nonferrous Met. Soc. China* **2019**, *29*, 2422–2429. [[CrossRef](#)]
16. Ye, W.; Xu, F.; Jiang, L.; Duan, N.; Li, J.; Zhang, F.; Zhang, G.; Chen, L. A novel functional lead-based anode for efficient lead dissolution inhibition and slime generation reduction in zinc electrowinning. *J. Clean. Prod.* **2021**, *284*, 124767. [[CrossRef](#)]
17. Wang, X.; Wang, J.; Jiang, W.; Chen, C.; Yu, B.; Xu, R. Facile synthesis MnCo<sub>2</sub>O<sub>4</sub> modifying PbO<sub>2</sub> composite electrode with enhanced OER electrocatalytic activity for zinc electrowinning. *Sep. Purif. Technol.* **2021**, *272*, 118916. [[CrossRef](#)]
18. Chen, S.; Chen, B.; Wang, S.; Yan, W.; He, Y.; Guo, Z.; Xu, R. Ag doping to boost the electrochemical performance and corrosion resistance of Ti/Sn-Sb-RuO<sub>x</sub>/α-PbO<sub>2</sub>/β-PbO<sub>2</sub> electrode in zinc electrowinning. *J. Alloys Compd.* **2020**, *815*, 152551. [[CrossRef](#)]
19. Zhang, F.; Zuo, J.; Jin, W.; Xu, F.; Jiang, L.; Xi, D.; Wen, Y.; Li, J.; Yu, Z.; Li, Z.; et al. Size effect of γ-MnO<sub>2</sub> precoated anode on lead-containing pollutant reduction and its controllable fabrication in industrial-scale for zinc electrowinning. *Chemosphere* **2022**, *287*, 132457. [[CrossRef](#)]
20. Gao, G.; Zhang, X.; Wang, P.; Ren, Y.; Meng, X.; Ding, Y.; Zhang, T.; Jiang, W. Electrochemical degradation of doxycycline hydrochloride on Bi/Ce co-doped Ti/PbO<sub>2</sub> anodes: Efficiency and mechanism. *J. Environ. Chem. Eng.* **2022**, *10*, 108430. [[CrossRef](#)]
21. Duan, P.; Qian, C.; Wang, X.; Jia, X.; Jiao, L.; Chen, Y. Fabrication and characterization of Ti/polyaniline-Co/PbO<sub>2</sub>-Co for efficient electrochemical degradation of cephalixin in secondary effluents. *Environ. Res.* **2022**, *214*, 113842. [[CrossRef](#)]
22. Shao, D.; Li, W.; Wang, Z.; Yang, C.; Xu, H.; Yan, W.; Yang, L.; Wang, G.; Yang, J.; Feng, L.; et al. Variable activity and selectivity for electrochemical oxidation wastewater treatment using a magnetically assembled electrode based on Ti/PbO<sub>2</sub> and carbon nanotubes. *Sep. Purif. Technol.* **2022**, *301*, 122008. [[CrossRef](#)]
23. Macounová, K.M.; Pittkowski, R.K.; Nebel, R.; Zitolo, A.; Krtil, P. Selectivity of Ru-rich Ru-Ti-O oxide surfaces in parallel oxygen and chlorine evolution reactions. *Electrochim. Acta.* **2022**, *427*, 140878. [[CrossRef](#)]
24. Preez, S.P.; Jones, D.R.; Warwick, M.E.A.; Falch, A.; Sekoai, P.T.; das Neves Quaresma, C.M.; Bessarabov, D.G.; Dunnill, C.W. Thermally stable Pt/Ti mesh catalyst for catalytic hydrogen combustion. *Int. J. Hydrog. Energy* **2020**, *45*, 16851–16864. [[CrossRef](#)]
25. Ma, D.; Ngo, V.; Raghavan, S.; Sandoval, S. Degradation of Ir-Ta oxide coated Ti anodes in sulfuric acid solutions containing fluoride. *Corros. Sci.* **2020**, *164*, 108358. [[CrossRef](#)]
26. Wang, Y.; Chen, M.; Wang, C.; Meng, X.; Zhang, W.; Chen, Z.; Crittenden, J. Electrochemical degradation of methylisothiazolinone by using Ti/SnO<sub>2</sub>-Sb<sub>2</sub>O<sub>3</sub>/α, β-PbO<sub>2</sub> electrode: Kinetics, energy efficiency, oxidation mechanism and degradation pathway. *Chem. Eng. J.* **2019**, *374*, 626–636. [[CrossRef](#)]
27. Chen, X.; Guo, H.; Luo, S.; Wang, Z.; Li, X. Effect of SnO<sub>2</sub> intermediate layer on performance of Ti/SnO<sub>2</sub>/MnO<sub>2</sub> electrode during electrolytic-manganese process. *Trans. Nonferrous Met. Soc. China* **2017**, *27*, 1417–1422. [[CrossRef](#)]
28. Hakimi, F.; Rashchi, F.; Ghalekhani, A.; Dolati, A.; Astarai, F.R. Effect of a synthesized pulsed electrodeposited Ti/PbO<sub>2</sub>-RuO<sub>2</sub> nanocomposite on zinc electrowinning. *Ind. Eng. Chem. Res.* **2021**, *60*, 11737–11748. [[CrossRef](#)]
29. Wang, Y.; Yang, C.M.; Schmidt, W.; Spliethoff, B.; Schüth, E.B.F. Weakly ferromagnetic ordered mesoporous Co<sub>3</sub>O<sub>4</sub> synthesized by nanocasting from vinyl-functionalized cubic Ia3d mesoporous silica. *Adv. Mater.* **2004**, *17*, 53–56. [[CrossRef](#)]
30. Alhaddad, M.; Ismail, A.A.; Alghamdi, Y.G.; Al-Khathami, N.D.; Mohamed, R.M. Co<sub>3</sub>O<sub>4</sub> nanoparticles accommodated mesoporous TiO<sub>2</sub> framework as an excellent photocatalyst with enhanced photocatalytic properties. *Opt. Mater.* **2022**, *134*, 112643. [[CrossRef](#)]
31. Dan, Y.; Lu, H.; Liu, X.; Lin, H.; Zhao, J. Ti/PbO<sub>2</sub> + nano-Co<sub>3</sub>O<sub>4</sub> composite electrode material for electrocatalysis of O<sub>2</sub> evolution in alkaline solution. *Int. J. Hydrogen Energy* **2011**, *36*, 1949–1954. [[CrossRef](#)]
32. He, S.; Xu, R.; Hu, G.; Chen, B. Electrosynthesis and performance of WC and Co<sub>3</sub>O<sub>4</sub> co-doped α-PbO<sub>2</sub> electrodes. *RSC Adv.* **2016**, *6*, 3362–3371. [[CrossRef](#)]
33. Tang, C.; Lu, Y.; Wang, F.; Niu, H.; Yu, L.; Xue, J. Influence of a MnO<sub>2</sub>-WC interlayer on the stability and electrocatalytic activity of titanium-based PbO<sub>2</sub> anodes. *Electrochim. Acta* **2020**, *331*, 135381. [[CrossRef](#)]
34. Wan, C.; Zhao, L.; Wu, C.; Lin, L.; Liu, X. Bi<sup>5+</sup> doping improves the electrochemical properties of Ti/SnO<sub>2</sub>-Sb/PbO<sub>2</sub> electrode and its electrocatalytic performance for phenol. *J. Clean. Prod.* **2022**, *380*, 135005. [[CrossRef](#)]

35. Zhu, Y.; Zhou, W.; Yu, J.; Chen, Y.; Liu, M.; Shao, Z. Enhancing electrocatalytic activity of perovskite oxides by tuning cation deficiency for oxygen reduction and evolution reactions. *Chem. Mater.* **2016**, *28*, 1691–1697. [[CrossRef](#)]
36. Kosmulski, M.; Mączka, E. Zeta potential and particle size in dispersions of alumina in 50-50 *w/w* ethylene glycol-water mixture. *Colloid. Surfaces A* **2022**, *654*, 130168. [[CrossRef](#)]

**Disclaimer/Publisher’s Note:** The statements, opinions and data contained in all publications are solely those of the individual author(s) and contributor(s) and not of MDPI and/or the editor(s). MDPI and/or the editor(s) disclaim responsibility for any injury to people or property resulting from any ideas, methods, instructions or products referred to in the content.